Fiber optic gyroscope technology

A.D. Kersey, A. Dandridge, and W.K. Burns

For over a decade, optical fiber-based interferometric techniques have been investigated for use in rotation sensing. Research began in the mid-1970s when the pioneering work of Vali and Shorthill[1] demonstrated for the first time the application of fiber optics for rotation sensing. This research effort, spawned in a number of laboratories worldwide,[2,3] was instrumental in bringing about significant advances in a number of component-related areas, especially in polarization maintaining (PM) fiber, PM fiber couplers, fiber polarizers, and sources. The performance of fiber optic gyroscopes improved over the years, with significant progress linked to a number of important developments, such as identification of the need for reciprocity and introduction of the super luminescent diode (SLD), which led to dramatic improvements due to the practical elimination of Rayleigh backscatter noise and drift due to the Kerr effect.

These and many other noteworthy advances have brought this technology from the realms of a laboratory curiosity to the point where rugged, compact fiber gyros are poised to compete with existing technologies for use in applications ranging from high-performance inertial navigational and long term platform stabilization systems to well-logging applications in the gas and oil exploration industry.

This article focuses on the principles of fiber optic gyroscope technology, the limitations to sensitivity due to noise and system imperfections, and research developments in the area of signal processing for improved dynamic range and stability.

Gyroscope configurations

All optical gyroscopes, including the ring laser and fiber gyroscope configurations, are based on the Sagnac effect, which produces a phase difference between two counterpropagating EM waves in a rotating frame of reference. The various types of optical gyros are as shown in Fig. 1. The two principle fiber gyroscope configurations of interest are the fiber 'Sagnac' or ring interferometer (com-

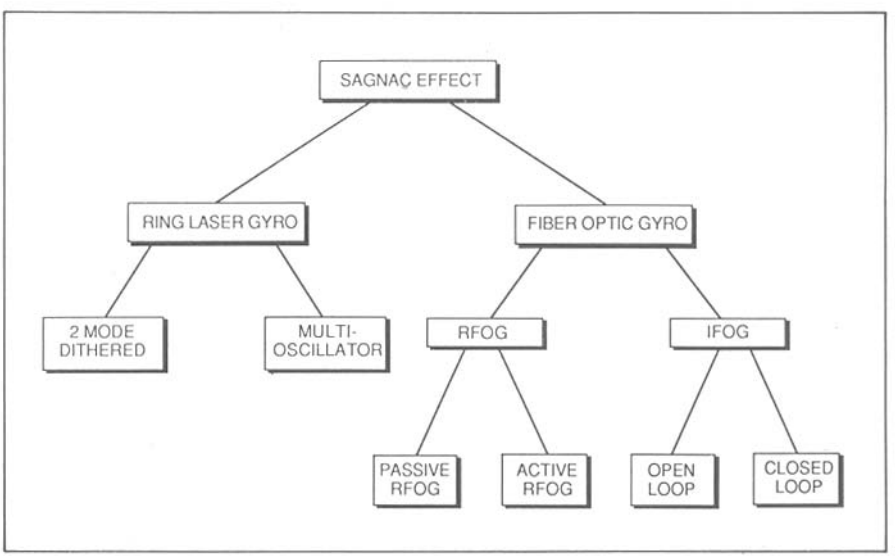

FIGURE 1. Optical gyroscopes based on the Sagnac effect.

A.D. KERSEY is a research physicist in the Optical Sensor Section headed by A. DANDRIDGE at the U.S. Naval Research Laboratory in Washington, D.C. W.K. BURNS heads the Optical Waveguide Section.

monly referred to as the interferometric fiber optic gyro or IFOG) and the fiber resonator (resonator fiber optic gyro or RFOG).

Figure 2 shows the basic optical configurations. In the Sagnac interferometer, light from an optical source is split into two components by a beamsplitter. These components are coupled into a fiber loop of N turns to form clockwise (CW) and counterclockwise (CCW) propagating optical fields. After passing through the fiber loop, the two optical components are recombined by the beamsplitter and the interference between them is detected at the ouput, as shown. In a rotating frame of reference, the Sagnac effect causes the effective optical path through the loop to increase for one beam, while for the other it becomes shortened. The resultant phase shift between the two optical components at the output is given by

$$2\phi_s = \frac{4\pi RL}{\lambda_0 c}\Omega. \qquad (1)$$

Here, R is the radius of the fiber coil, L is the total length of fiber in the loop, λ_o is the vacuum wavelength of the source radiation, c is the velocity of light, and Ω is the rotation rate. The phase $2\phi_s$ is known as the Sagnac phase shift. As an example of the magnitude of this effect, a 1000 turn fiber coil of 20 cm diameter rotating at 1°/hr produces a Sagnac phase shift of approximately 10^{-5} radians for an optical source of wavelength ~ 1 μm. Consequently, the measurement of rotation rates on the order of 0.01°/hr^{-7} using such a gyro requires a phase shift detection sensitivity of $\sim 10^{-7}$ radians, or a relative change in optical path length of the fiber coil of one part in 10^{17}—a very demanding task.

To achieve this degree of accuracy, the two paths experienced by the two optical beams must be identical when the gyro is in a non-rotating frame—that is, the system must exhibit reciprocity. The so-called "minimum configuration" of the optical system

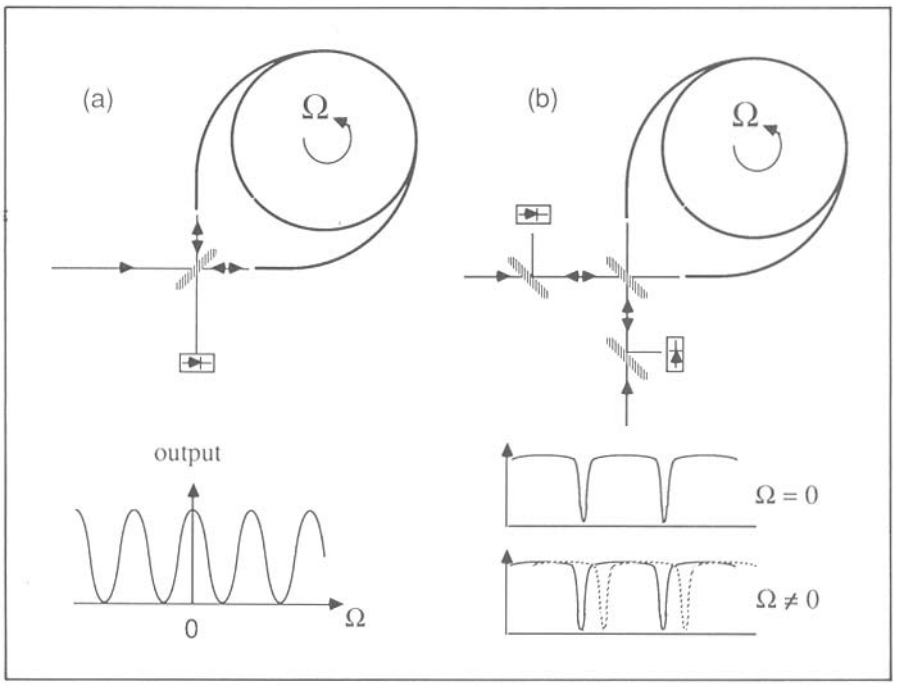

FIGURE 2. Basic optical configuration of the Sagnac interferometer and Ring resonator.

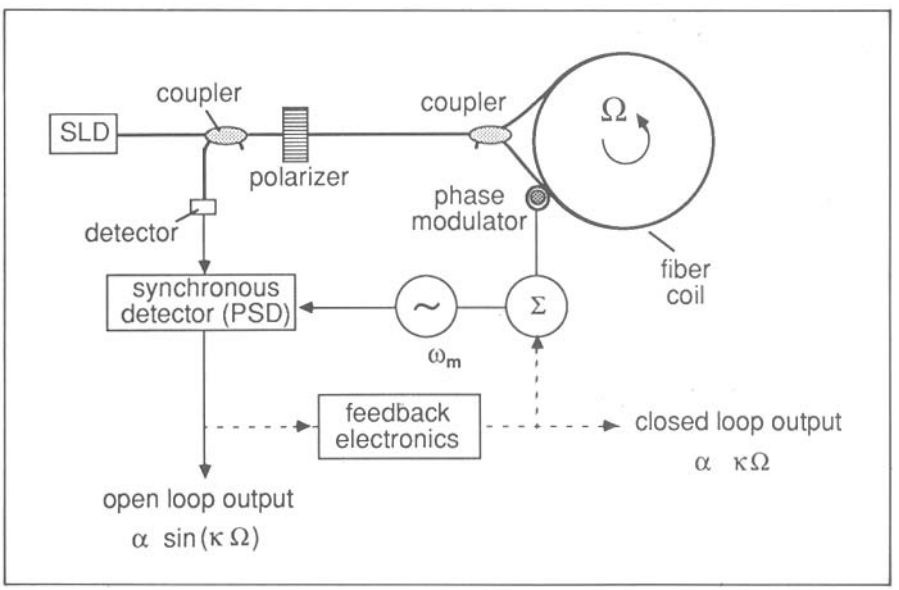

FIGURE 3. Minimum configuration for an interferometric fiber gyroscope showing open and closed loop configurations.

required to achieve this is shown in Fig. 3. Here, the output is derived from the same coupler port that is used as the input (via a second coupler) and a polarizer is used at the input to the fiber loop. This is required to ensure that single spatial mode, single polarization mode operation is achieved to satisfy requirements for reciprocity in the fiber loop. The output of the Sagnac interferometer, as shown in Fig. 1, is a cosine interfer-

ence function of the form or

$$S = 1 + \cos(\phi_{nr} + 2\phi_s) \qquad (2)$$

where ϕ_{nr} is a nonreciprocal phase shift, and $2\phi_s$ is the rotation induced Sagnac phase. For a reciprocal system, $\phi_{nr}=0$ and the sensitivity to Sagnac shift $\partial S/\partial(2\phi_s) = 0$, whereas if $\phi_{nr} = \pi/2$, the sensitivity is maximized.

A number of mechanisms can be used to introduce a nonreciprocal phase shift. The most commonly used approach is known as dynamic phase biasing, where a time varying modulation $\phi_{nr} = \phi_m \sin\omega_m t$ is applied via a phase shifter located at one end of the gyro coil. With the gyro in stationary frame, the time varying nonreciprocal phase bias modulates the interferometer output symmetrically over the cosine interferometer transfer function described by Eq. (2). In a rotating frame, however, the Sagnac phase shift introduces an offset that causes an asymmetric output modulation. The component in the detected output at the fundamental of the modulation frequency is then

$$S(\omega_m) = J_1(\phi_m) \sin(2\phi_s) \qquad (3)$$

The optimum modulation frequency ω_m is known as the "proper" or "eigen-frequency" of the loop and is given by $\omega_m = \pi/\tau$, where τ is the propagation time for light through the fiber coil. There are two basic modes of operation of the IFOG: open-loop and closed-loop. Figure 3 shows schematically the basic configurations used to implement the two modes. In the first, the magnitude of Sagnac phase shift is determined directly by measurement of $S(\omega_m)$; in the second, $S(\omega_m)$ is nulled by feedback to the fiber coil using frequency or phase modulators to introduce a nonreciprocal phase to counter-balance the Sagnac shift.

In the resonator fiber optic gyroscope configuration, a fiber cavity is used to sense rotation-induced Sagnac phase shifts. This basic concept is shown in Fig. 1(b). The fiber resonator is formed by the coil and a high reflectance beamsplitter and has a transmission function characterized by sharp dips, analogous to a Fabry-Perot interferometer in reflection. The configuration has two input ports that give rise to CW and CCW recirculating modes in the fiber coil. In a non-rotating frame, the eigen-frequencies of the input optical frequency at which the dips in the transmission function occur is the same for both input ports. However, when a Sagnac phase shift is introduced, these eigen-frequencies become non-degenerate, with the difference being directly proportional to the rotation rate.

In general, the RFOG is optically interrogated at both inputs from a common optical source using frequency shifters such as acousto-optic modulators (AOM) to track the eigen-frequencies f_{cw} and f_{ccw}, as shown in Fig. 4. The output is then simply derived by monitoring the beat frequency $\{f_{cw}\text{-}f_{ccw}\}$, as shown. The RFOG has the advantage over the IFOG of requiring less fiber in the sensing coil, but has many significant drawbacks, including the requirement of a highly coherent source and very low-loss fiber components.

Of the two gyroscope configurations, the IFOG is presently far more highly developed, with several companies actively engaged in the commercialization of systems developed in recent years.

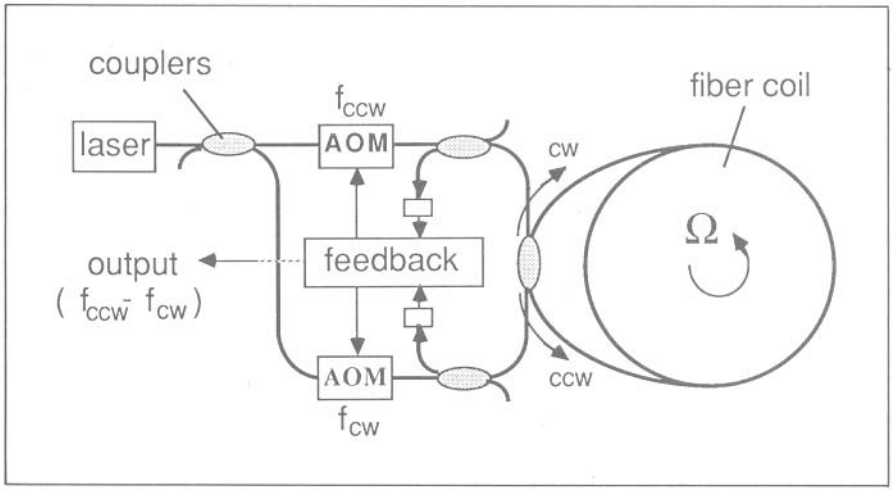

FIGURE 4. Gyroscope based on the ring resonator.

Sources of noise and drift

The fundamental limit to the rotation rate detection sensitivity of a fiber gyroscope is determined by the quantum limited shot noise, or photon noise. This, of course, is a function of the input optical power coupled to the device, the intrinsic attenuation of the fiber, the length of fiber used, and the radius of the fiber coil. Analysis shows the shot noise limited resolution is given by

$$\Omega_{min} = \frac{kc\lambda_0}{4\pi LR}\left[\frac{Bq}{DP_d}\right]^{1/2} \qquad (4)$$

where, B is the detection bandwidth, $P_d=(1/4)P_o \exp(-\alpha L/4.3)$ is the peak power incident on the detector, α is the loss coefficient of the fiber in dB/m, D is the responsivity of the optical detector in A/W, q is the electronic charge, and $k \approx 2.3$ is a factor that accounts for the bias modulation. For a practical system based on a fiber coil of length 1 km wound on a 5 cm radius, and input power of 1 mW at a wavelength of 1.3 μm (D~ 0.77 A/W

The fundamental limit to the rotation rate detection sensitivity of a fiber gyroscope is determined by the quantum limited shot noise . . .

is assumed), we have a shot-noise equivalent rotation rate

$$\Omega_{min} \approx 10^{-2}\ ^\circ/\text{hr}. \qquad (5)$$

in a 1 Hz bandwidth. This corresponds to a random drift or random walk coefficient (RWC) of

$$\text{RWC} \approx 2.10^{-4}\ ^\circ/\text{hr}.^{1/2} \qquad (6)$$

Figure 5 shows the dependence of the random drift (RWC) on the length of fiber, L, for various source wavelengths, a coil radius of 5 cm, and an input optical power level of 1 mW. These calculations take into account the different fiber attenuation coefficients and detector responsivities at the three wavelengths considered. As can be seen, the optimum fiber length is several km to tens of km.

While this limit to the rotation accuracy of a fiber gyroscope would be adequate for many practical applications, it is informative to note that by increasing R by one order of magnitude and using the optimum length of fiber for 1.3 μm, a shot noise limit to the RWC of $\sim 10^{-5}$°/hr.$^{1/2}$ could be achieved. This degree of accuracy could be required in some of the most demanding application areas for IFOG technology, such as long term, spacecraft stabilization.

In practice, other noise sources, such as those arising due to environmental perturbations of the gyro coil, optical backscatter, time varying nonreciprocal effects, polarization noise, source instabilities, and electronic noise and drift, may limit the performance of a fiber gyroscope.

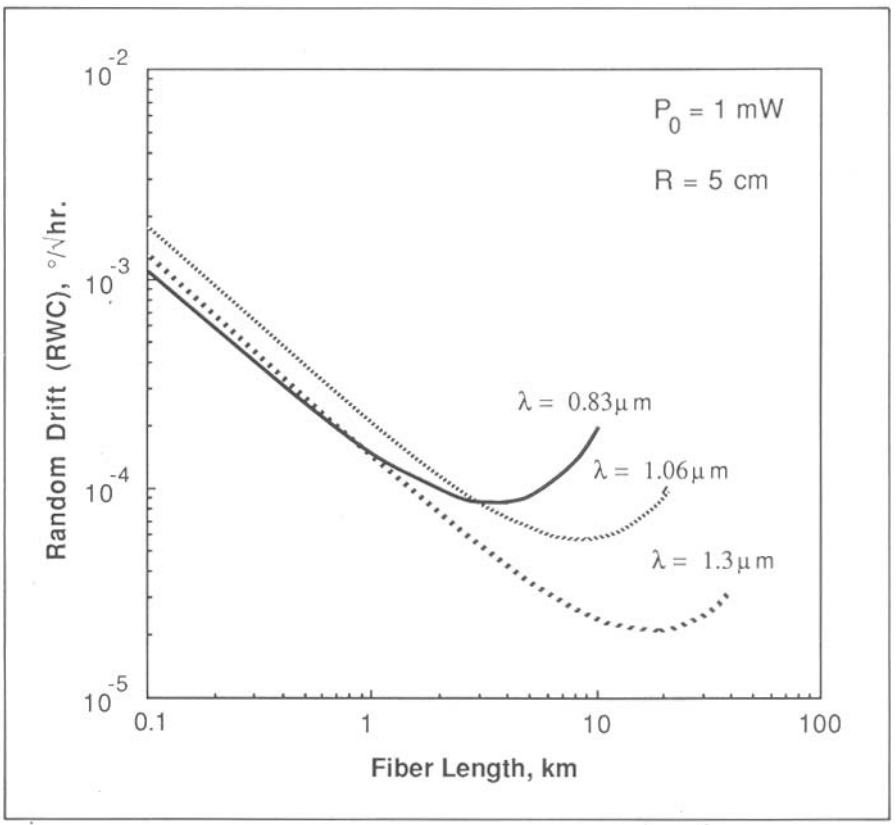

FIGURE 5. Theoretical shot noise limited random drift in an IFOG for various wavelengths.

The Faraday effect is a magnetically induced rotation of the optical polarization and is a nonreciprocal effect. Since the effect is indistinguishable from a Sagnac signal, it results in noise and drift at the gyro output. Both magnetic shielding of the fiber coil and polarization maintaining fiber have been used to reduce drift due to the Faraday effect.

An additional source of nonreciprocity is the Kerr effect, a nonlinear optical effect related to four-wave mixing, which gives rise to an optical intensity induced nonreciprocal effect. In a fiber gyroscope, when the intensities of the counterpropagating beams become unequal, the propagation constants for the two beams become unequal. As with the Faraday effect, this causes a nonreciprocal phase shift indistinguishable from a Sagnac phase shift. However, this source of drift can be greatly reduced by using a broadband source, such as a superluminescent diode. When summed over all the wavelength components of such a source, the Kerr-induced phase shift averages to zero.

Another source of nonreciprocal operation can arise due to polarization mode coupling in a fiber coil. Conventional single mode fiber actually supports two nearly-degenerate polarization modes with slightly different optical propagation constants. Coupling between these modes can occur due to bends or jacket pressure. When one beam travels one path between the two polarization modes and the counter-rotating beam travels a different path, nonreciprocal opera-

tion occurs. Because coupling points can vary in a rapid random fashion due to thermal and mechanical fluctuation in the fiber coil, this process can lead to noise at the gyro output. The most straightforward way to alleviate this problem is by using polarization maintaining fiber in the gyro coil.

Rayleigh backscattering in the fiber coil also leads to a source of noise. The discovery of this noise source was an important step in the development of high performance gyroscopes, as it improved gyro sensitivities from the degree per second range to the degree per hour range. Rayleigh backscattering occurs due to microscopic variations in refractive index that occur along a fiber. The net backscatter signal is due to a coherent summation of components from individual scattering centers along the fiber. Because of acoustic and thermal perturbation of the fiber, the backscatter intensity can be a rapidly time-fluctuating quantity.

In a fiber gyro, backscattered signals mix with the counter-rotating optical beams and lead to an output signal that again is indistinguishable from a Sagnac phase shift. Rayleigh backscattering can be overcome by using a source of short coherence length, such as provided by a multimode diode laser or SLD.

Signal processing for the IFOG

Most systems in the early/mid-1980s used the open loop mode of operation, where the rotation-induced Sagnac phase shift is detected by monitoring the resulting shift in the output interference pattern of the device. In laboratory breadboards, this approach has achieved the highest sensitivities in terms of bias drift rate and random walk coefficient. The output of the open-loop gyroscope is, however, proportional to the source intensity and phase modulator drive level. This gives rise to an increased possibility of variation in the gyro scale factor (gyro output/rotation rate). The dynamic range of the open loop gyro is also limited by the sinusoidal nature of the interference output.

A number of techniques that address the limitations of the basic open loop approach have been developed in recent years. These schemes address the biasing, dynamic range, and scale factor stability issues in different ways using modified open-loop signal processing or some form of closed loop approach. Forms of passively "optically-biased" open loop schemes have been developed, based on 3 × 3 fiber couplers, or the use of dual polarization modes within the fiber coil. The dynamic range problem has been addressed in open loop configurations by adopting synthetic heterodyne demodulation techniques, dual wavelength interrogation and amplitude (modulation) switched techniques.

Synthetic heterodyne phase detection is an interesting approach to open loop processing that can be used to overcome the dynamic range limitation of the basic open-loop/synchronous detection scheme. In this approach, the Sagnac phase shift is transposed into the relative phase of a low-frequency electrical carrier signal, which can be "demodulated" using phase-tracking techniques. These variant open loop schemes offer solutions to the limitations of the basic approach that may be suitable for use in many low-cost gyro systems, especially in relatively low-accuracy (0.1–1%) rate sensing applications.

In contrast to open loop systems, closed loop gyroscope configurations offer the potential of high performance rotation rate sensing with low drift, wide dynamic range, and high scale factor stability. Closed loop signal processing is, however, considerably more complex, both optically and electronically, typically involving high speed digital electronics.

The principle of the original closed loop or "phase nulling" gyroscope was based on frequency shifting the

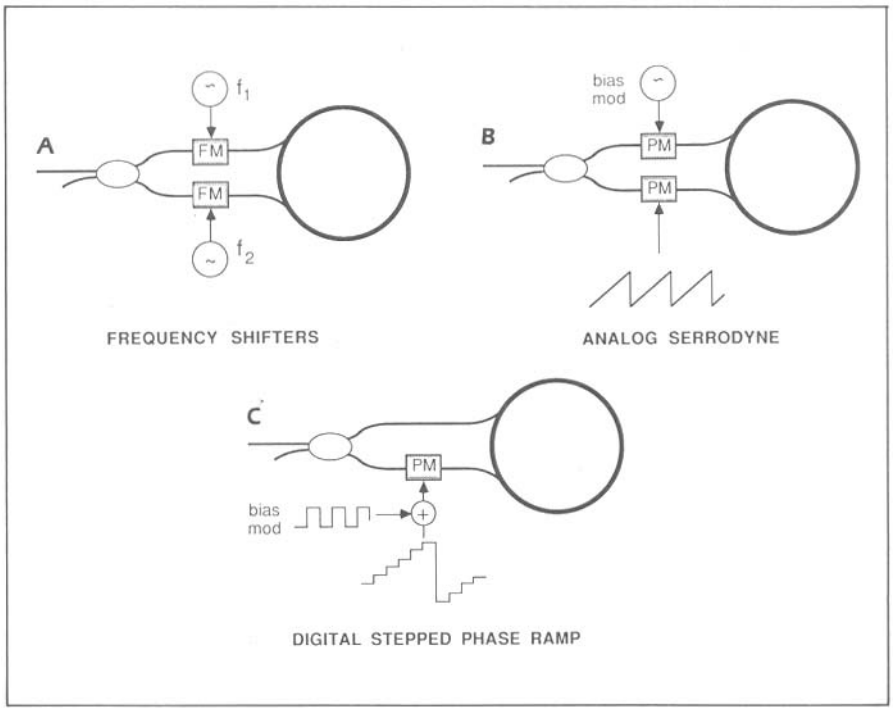

FIGURE 6. Closed loop IFOG signal processing techniques: a) frequency shifters, b) analog serrodyne ramp, c) digital phase-stepped ramp.

CW and CCW counterpropagating beams in a Sagnac interferometer using bulk-optic acousto-optic frequency modulators. A schematic of the configuration typically used is shown in Fig. 6 (a). Before being coupled into the fiber coil, the CW propagating light is frequency offset by ω_1 and the CCW light by ω_2. At the output of the fiber coil, the CW propagating light is then frequency offset by ω_2 and the CCW light by ω_1, such that the two components experience an equal net frequency shift.

It can be shown that in the absence of any additional nonreciprocal phase shift, the phase difference between the two components is given by

$$\Delta\psi = \Delta\omega n L/c \qquad (7)$$

where $\Delta\omega = (\omega_1 - \omega_2)$, and n is the effective index of the fiber. This phase difference is directly proportional to the frequency offset $\Delta\omega$ between the CW and CCW counterpropagating beams and can be used to compensate for rotation-induced Sagnac phase shifts in the interferometer. The output is then given by $\Delta\omega$. Using equations (2) and (6), the relationship between rotation and frequency offset $\Delta\omega$ is given by

$$\Delta f = \frac{\Delta\omega}{2\pi} = \frac{2R\Omega}{\lambda n} \qquad (8)$$

As an example of the magnitude of frequency shift required, a rotation of 1°/hr corresponds to a Δf of approximately 0.5 Hz for a gyro coil of 10 cm radius operating at a wavelength of ~1.3μm. A dynamic range of 2×10^6 (max rate of ± 500°/s) would require a frequency shift capability of approximately ± 1 MHz. This form of frequency output is particularly desirable for rate integrating, as counting the number of cycles is directly proportional to the angular position of the gyroscope coil. The major disadvantages of the approach are due to the non-all-fiber construction, which introduces stability and alignment issues, and the dependence of $\Delta\omega$ on n, which introduces a source of scale factor drift due to the temperature dependence of refractive index.

The principle advantages of fiber optic gyros include solid-state operation (no moving parts), light weight, small size, low power, rapid turn-on time, and high reliability.

More recently, emphasis has shifted to the use of integrated optic waveguide phase modulators. These components integrate well with the fiber loop and operate based on serrodyne frequency translation or digital phase stepping techniques to compensate for the rotation-induced Sagnac phase shift. Although the use of integrated optic frequency translation in the phase nulling gyroscope was proposed at an early stage in gyro development, implementation has only been demonstrated with success in the last few years. In this case, the frequency shift is obtained by serrodyne modulation (sawtooth or ramp function) applied to an integrated optic phase modulator, as shown in Fig. 6(b). For a serrodyne modulation with an infinitely fast flyback time, a phase modulation of 2πp-p at a rate f_r is equivalent to an optical frequency shift equal to f_r. In practice, the finite reset time and nonlinearity in the modulation function limit the degree with which this can be accomplished. Consequently, spurious weak components are generated at harmonics of f_r, which can lead to scale factor nonlinearities. Work on serrodyne modulators and drivers with fast flyback times (≤ 10 nS) have produced sideband suppression ratios as high as 56 dB.

The latest developments in closed loop gyroscope technology has been in the use of digital phase stepping ramps to null the Sagnac phase shift. Because of the finite propagation time, τ, of light through a fiber coil, a step change in optical path length at one end of the coil is a nonreciprocal event for a period τ, after which point the effect is cancelled. This can be used to offset the Sagnac phase shift experienced by the counterpropagating beams in the gyro coil. To accomplish this, a continuous phase stepping ramp (staircase waveform) is applied to a phase modulator, with each step of duration τ, and amplitude $\Delta\phi$ equal to the Sagnac phase shift. This principle of operation is shown in Fig. 6(c).

To monitor the phase of the interferometer, an additional biasing phase modulation can be applied to the system. This is extremely straightforward in this approach, as the proper modulation frequency is $1/2\tau$—synchronous with the phase stepping ramp. The two waveforms can, therefore, simply be added at the phase modulator. Using the phase stepping to compensate for the Sagnac phase shift necessitates resetting the phase modulation when the limits of the modulator are reached, or more typically when the phase stepping has reached $\pm 2\pi$ rad. The number of phase steps between resets is a precise measure of the step size, and thus the Sagnac phase shift. Furthermore, as in the analog-ramp closed loop schemes, digital rate integration is acquired through counting the number of resets.

Applications and performance

The principle advantages of fiber optic gyros include solid-state operation (no moving parts), light weight, small size, low power, rapid turn-on

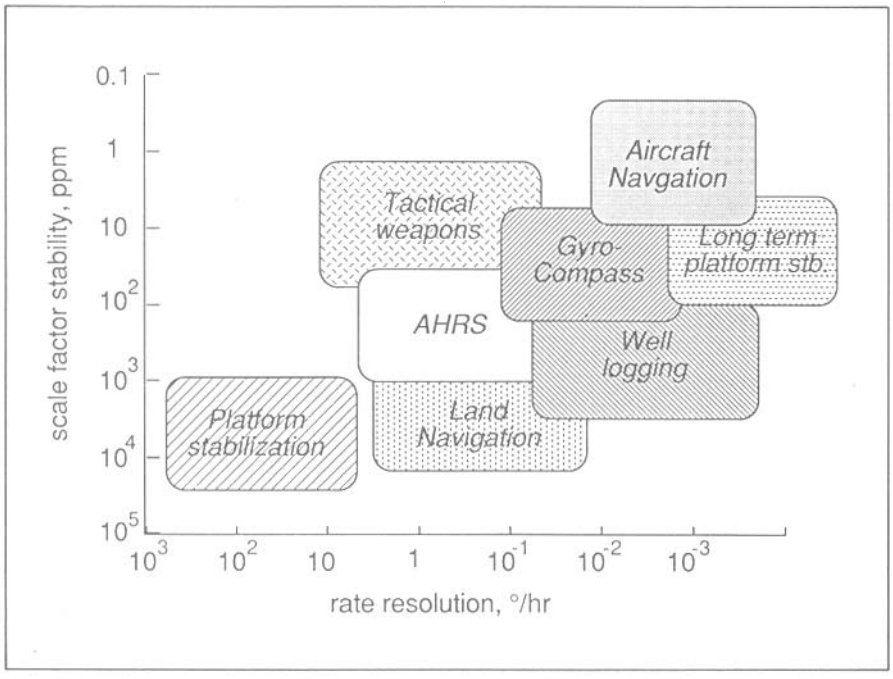

FIGURE 7. Application areas and drift rate/scale factor stability requirements for fiber optic gyro technology.

time, and high reliability. Consequently, fiber gyros have been proposed for rotation sensing in a wide range of application areas. Figure 7 shows the required bias drift and scale stability for a number of the potential application areas for fiber gyros. Much of the research has been directed toward the development of aircraft inertial navigational grade gyros with bias drift ~0.01°/hr or less. The scale factor requirement for this application is ~10 ppm or better, which is the level currently being attained by a number of closed loop gyro systems.

Interest has also been directed at a number of other application areas, such as attitude and heading reference systems (AHRS) for use in inertial measurement units (IMU), land-based navigation, and well logging for use in the oil and gas exploration industry. One area being explored in land navigation is the development of low cost low-medium accuracy devices for automobile guidance/tracking systems. Lower accuracy systems can be used in such applications, as positional updates from GPS (satellite) or ground-based referencing can be used to augment the system. Hitachi in Japan has demonstrated a prototype gyro with a resolution of ~0.01°/s and an accuracy of < 0.25% for rotations < 70°/s for this application.[5]

Table I summarizes the research interests of a number of laboratories and companies actively engaged in fiber optic gyroscopes. Emphasis is clearly being directed toward the development of closed loop systems with scale factor stabilities of ~100 ppm or better. However, open loop technology may still find use in applications where moderate scale factor stabilities are sufficient. Honeywell has a 3-inch diameter open loop device slated for production in the near future, and recent work at NRL has identified and characterized sources of scale factor errors in open loop systems.

As seen in Table I, Honeywell, JPL,

Several of the current problem areas associated with fiber optic gyros appear to have relatively near-term technical solutions.

Litton, Smiths, and Thomson CSF (France) are engaged in the development of sophisticated closed loop gyro systems for applications such as aircraft inertial navigational systems. Recent work reported by Honeywell on a 7-inch closed loop breadboard gyro has produced some of the best scale factor data reported to date—a scale factor linearity of 30 ppm and reproducibility better than 10 ppm.[6]

Both Litton and Smiths are developing gyros based on approximately 1.5 inch fiber coils for use in a 3-axis rotation sensor in IMUs. A novel form of signal processing for use with the closed loop serrodyne approach has been developed by researchers at the Jet Propulsion Laboratory (JPL). An auxiliary interferometer is formed by tapping a small amount of light from the CW and CCW beams before they are injected into the fiber coil. This permits optical detection of 2π phase excursions induced by the serrodyne modulator.

Research and development is also being conducted at a number of other industrial laboratories, including United Technologies, British Aerospace, Phonetics S.A.(France), JAE in Japan, and Standard Electrik Lorenz (SEL) in the Federal Republic of Germany. SEL recently conducted temperature and shock testing of a number of identical prototype gyros with ~10°/hr performance. Both British Aerospace and Phonetics have recent-

ly developed advanced prototype, medium accuracy gyros for use in AHRS applications.

Future trends

Several of the current problem areas associated with fiber optic gyros appear to have relatively near-term technical solutions. Issues of superluminescent diode source reliability, availability, and cost have long been a problem for gyro developers. The wavelength stability of these sources has also been poorer than lasers, leading to scale factor drifts with temperature and time. For high accuracy gyros, these effects have necessitated wavelength monitoring and active wavelength control or periodic scale factor re-calibrations. High sensitivity gyros require high optical power levels that tend to shorten source lifetimes.

One development that may have a major impact on this situation is the recent availability of Nd-doped fiber sources that can be laser diode-pumped and run in a superfluorescent mode to achieve high power and broadband output. These sources are well suited to integration, appear to have at least an order of magnitude improvement in wavelength stability compared to SLDs, and when pumped with a diode laser array or broad stripe laser, are capable of tens of milliwatts of output power.

Another area of potential concern has been DC drift and photorefractive instabilities in Ti-diffused $LiNbO_3$ integrated optical circuits used in closed loop IFOGs. Although the most successful signal processing schemes have used feedback loops to alleviate the effects, they still remain a fundamental limitation, particularly as higher power sources become available. Recent improvements in the performance of hydrogen diffused (proton exchange) $LiTaO_3$ integrated optical circuits promise to largely eliminate photorefractive effects as a drift source. These devices have demonstrated high power handling capability, are low loss, electro-optically stable, and automatically provide a polarizing function. The use of Nd-doped fiber sources at 1.06 μm will also aid in the reduction of photorefractive effects due to the increase in wavelength from 0.83 μm GaAlAs SLD wavelength most commonly used at present.

Fiber optic gyros offer solid state, reliable, high performance rotation sensing for a wide range of applications.

Fiber optic gyros offer solid state, reliable, high performance rotation sensing for a wide range of applications. The major sources of noise and drift have been overcome and emphasis has turned to issues concerning packaging, environmental sensitivity, and scale factor stability. Several companies are currently engaged in the testing of advanced, pre-production versions of fiber gyros. In general, research and development in fiber optic gyros over the past several years has proven the technology to be viable for the next generation of solid state rotation sensors.

REFERENCES

1. V. Vali and R.W. Shorthill, *Fiber ring interferometer*, Appl. Optics, **15**, p. 1099, 1976.
2. See: *Fiber Optic Rotation Sensors and Related Technologies*, Springer Series in Optical Sciences Vol. **32**, S. Ezekiel and H.J. Arditty (eds.), N.Y., Springer Verlag, 1982.
3. See: *10th Anniversary Conference on Fiber Gyros*, SPIE Proc. Vol. **719**, Cambridge, Mass., 1986.
4. R.A. Bergh, H.C. Leferve, and J.H. Shaw, *Overview of fiber-optic gyroscopes*", IEEE J. Lightwave Technology, LT-2, p. 91, 1984.
5. T. Sasayama et. al., *Recent developments of optical fiber sensors for automotive use*, SPIE Proc. Vol. **840**, p. 37, San Diego, Calif., 1987.
6. R.Y. Liu et al., *Progress toward an intertial grade fiber optic gyroscope*, Proc. Nat. Technical Meeting of the Institute of Navigation, San Mateo, Calif., January 1989.

	Configuration	Operation	bias drift	Comments
Andrew Corp	Open-loop IFOG	PM fiber and components, p/z modulator	~ .01 °/hr	in-house PM fiber, couplers and polarizers
Draper Lab.	RFOG	All fiber resonant cavity with input frequency shifters	—	—
Honeywell	Open & closed-loop IFOGs	Analog serrodyne closed loop system	~ .3 °/hr (o.l.) ~ .02 °/hr (c.l.)	High scale factor stability (<10 ppm) demonstrated with closed loop approach
JPL	Closed-loop IFOG	Analog serrodyne closed loop system	—	JPL/AT&T research Optical detection of serrodyne resets
Litton	Closed-loop IFOG	Digital serrodyne closed loop IFOG	.01 °/hr	High scale factor stability (~ 10 ppm) demonstrated
NRL	Open-loop IFOGs	i) low bias drift PM based FOG with p/z modulator; ii) wide dynamic range	.005 °/hr	high performance open loop gyro.
Stanford U.	Open-loop IFOGs	open loop wide dynamic range systems Fiber sources	—	—
Smiths	Closed-loop IFOG	Closed loop IFOG systems	~ .5 °/hr	non-PM based gyro Polarization insensitive IOC modulator
Thomson CSF	Closed-loop IFOG	Digital phase stepping closed loop IFOG	~ .3 °/hr	High speed digital signal processing

TABLE 1. Current research efforts in fiber optic gyroscope technology.